The Double Gaussian Distribution of Inhomogeneous Barrier Heights in Al/GaN/p-GaAs (MIS) Schottky Diodes in Wide Temperature Range

S. Zeyrek[1]*, M. M. Bülbül[2], Ş. Altındal[2], M. C. Baykul[3], and H. Yüzer[4]
[1]*Department of Physics, Faculty of Arts and Sciences, Dumlupınar University, 43100, Kütahya-Turkey*
[2]*Department of Physics, Faculty of Arts and Sciences, Gazi University, 06500, Ankara–Turkey*
[3]*Department of Physics, Osmangazi University, 26480, Eskişehir-Turkey*
[4]*Material and Chemical Technologies Research Institute,*
Marmara Research Center, P.O. Box 21, 41470 Gebze-Kocaeli, Turkey

The current-voltage (I-V) characteristics of metal-insulator-semiconductor (Al/GaN/p-GaAs) Schottky barrier diodes (SBDs) were investigated over a wide temperature range of 80-380 K. By using the thermionic emission (TE) theory, the zero bias barrier height Φ_{B0} calculated from I-V characteristics was found to increase with increasing temperature as the ideality factor n decreases with increasing temperature, and especially the activation energy plot is nonlinear at low temperatures. The observed variation in the Φ_{B0} and n is attributed to the spatial barrier inhomogeneities in SBD by assuming a Gaussian distribution (GD) of barrier heights (BHs). The experimental I-V-T characteristics of the SBDs have shown a double Gaussian distribution having mean barrier heights $\bar{\Phi}_B$ of 0.854 eV and 0.395 eV and standard deviations σ_s for 0.142 V and 0.059 V, respectively. The modified $\ln(I_o/T^2)-q^2\sigma_o^2/2(kT)^2$ vs q/kT plot gives Φ_{B0} and Richardson constant A^* as 0.858 eV and 0.364 eV, and 78.5 and 128 A/cm^{2}K^2, respectively, without using the temperature coefficient of the barrier height. Hence, the results have shown that the I-V-T characteristics of the Al/GaN/p-GaAs SBDs can be successfully explained on the basis of TE mechanism with a double Gaussian distribution of the barrier heights.

Keywords: MIS diode; Barrier inhomogeneities; Double Gaussian distribution; Temperature; Dependence; Nitride passivation

1. INTRODUCTION

Metal-semiconductor (MS) and metal-insulator-semiconductor (MIS) Schottky barrier diodes (SBDs) play a very important role in the micro electronic devices. These type devices have important application in a wide variety of the optoelectronic, bipolar integrated circuits and high frequency applications. There are currently a vast number of experimental studies on diode characteristics parameters such as Schottky barrier heights (SBHs), ideality factor n, series resistance R_s and surface states N_{ss} in a great variety of MS and MIS type SBDs [1-17]. The performance and reliability of these devices especially depends on formation of insulator layer between metal and semiconductor interface, the density of interface states distribution between semiconductor and insulator layer, series resistance and inhomogeneties of Schottky barrier contacts.

The characterization of a SBD with an interface layer does not obey the ideal Schottky theory. Especially understanding Schottky barrier formation between metal and semiconductor interface on a fundamental basis still remains a challenging problem. Also, Schottky barrier height, and ideality factor are the fundamental parameters of the MS or MIS structures and strongly effected devices performance.

Also, in a broad temperature range or at room temperature current-voltage (I-V) measurements alone do not provide detailed information about the nature of barrier formation between metal and semiconductor and current-transport mechanisms. The analysis of the I-V characteristics of MS or MIS SBDs at wide temperature range allows us to understand different aspects of barrier formation and current-transport mechanisms [9,15-18]. In general, the I-V-T characteristics of SBDs based on Thermionic Emission (TE) usually reveal an abnormal increase in the SBH and a decrease in the ideality factor n with decrease in temperature [9,18-20]. In addition, the decrease in the BH at low temperatures leads to non-linearity in the activation energy plot ln (I_o/T^2) vs 1/T plot. This abnormal behaviour of SB at low temperature has been attributed to be the spatial variation of BHs in the Al/GaN/p-GaAs (MIS) Schottky diodes. Recently, the spatial barrier homogeneities in MS and MIS type SBDs are described mainly by a Gaussian distribution function and is widely used to explain the experimental I-V characteristics [11,16, 20,22,23].

Gallium arsenide is one of the advantageous semiconductors for high-speed and low-power devices [1]. The formation of a direct on GaAs by traditional ways oxidation or deposition cannot completely passivate the active dangling bonds at the semiconductor surface. Thus, various non-traditional approaches for surface passivation sulfide, selenide layer and nitride formation have been a subject of increasing interest in recent years [37-48,50].

As known, nitrides are very stable against oxidation. Therefore, one can expect that the nitride layers should prevent the formation of amorphous surface oxides on the GaAs at atmospheric ambient. Also, due to a high value of their electronegativity (3.04) nitrogen atoms bonded with surface gallium should not produce electronic states in the forbidden gap [24]. However, it has been reported that the passivated surface of GaAs is quickly degraded when it was exposed to air ambient. Due to the formation of many kind sub-oxides of both Ga and As, the control of the chemical composition in the GaAs oxide is very difficult [21]. In contrast, gallium nitride (GaN) is an excellent widegap III-V compound semiconductor because of its thermal and chemical stability [45].

————
*E-mail address: szeyrek@dumlupinar.edu.tr

As known, there are many techniques for nitridation process. Electrochemical anodization technique is an economical and practical way to produces a very thin film on the GaAs substrate [17,37-40,50]. We used same technique in our previous work, too [17].

We present, in this work, non-aqueous ammonium polynitride $((NH_4)_2(NH_2)_x)$ electrolyte was employed to grow a Gallium nitride layer on the GaAs surface as a new method of nitride passivation. Nitridation of GaAs surface was also performed by electrochemical anodization technique. The I-V characteristics of Al/GaN/p-GaAs SBDs were investigated over a wide temperature range of 80-380 K. The temperature dependence of barrier height (SBHs) characteristics of Al/GaN/p-GaAs (MIS) diodes were interpreted on the basis of the existence of Gaussian distribution of the BHs around a mean value due to barrier height inhomogeneities prevailing at the metal-semiconductor interface.

2. EXPERIMENTAL PROCEDURE

Al/GaN/p-GaAs (MIS) Schottky barrier diodes were fabricated on 2 inch diameter float zone (100) p-type (Zn doped) single crystal GaAs wafer having thickness of 280 μm. The sample was ultrasonically cleaned in trichloroethylene and ethanol, etched by $H_2SO_4/H_2O_2/H_2O$=5:1:1 (weight ratio) solution for 30 s., rinsed by propylene glycol and blown with dry nitrogen gas. The back contacts of the electrodes were formed by evaporating Al in high vacuum (P=10^{-6} Pa) and subsequently to form ohmic contact annealing them for a few minutes at 450 ^oC. After making of electrical contact, the walls and under side of the GaAs wafer were insulated with the high-quality wax. The nitridation set-up, using in the study is the electrochemical anodization cell which consists of a p-GaAs anode and Pt cathode. An agitation of the electrolyte is achieved by magnetic stirrer. Electrolyte used in the experiment was obtained by sequentially mixing of propylene glycol with ammonia (NH_3) and hydrazine (NH_2-NH_2) at 21:3:1 weight ratio, respectively. Preceding each of cleaning step, the wafer was rinsed thoroughly in de-ionized water with resistivity of 18 MΩcm.

Immediately after that, the substrate was immersed in electrolytical cell. Anodic nitridation was performed using a constant current source at different current densities, under light and N_2 flow, at room temperature (293 K). The potential difference between the electrodes normalized to calomel electrode was measured with an x-t recorder. The anodization was stopped, when the cell voltage reached about the 25 V. After, the sample was immediately rinsed in propyl alcohol and blown dry nitrogen and left in a desiccators. The Schottky contacts were formed by evaporating of Al dots with diameter of about 1.0 mm and 2500 Å thick in high vacuum (P=10^{-6} Pa). The metal thickness of layer and the deposition rates were monitored with the help of quartz crystal thickness monitor. In this way, metal-interfacial insulator layer-semiconductor (Al/GaN/p-GaAs) MIS Schottky barrier diodes were fabricated on p-type GaAs wafer. The interfacial insulator layer thickness (GaN) was estimated to be about 63 Å from mea-

surement of the insulator capacitance in the strong accumulation.

The current-voltage (I–V) measurements were performed by the use of a Keithley 220 programmable constant current source, a Keithley 614 electrometer. I-V characteristics were measured in the temperature range of 80-380 K using a temperature controlled Janes vpf-475 cryostat, which enables us to make measurements in the temperature range of 77-450 K. The interfacial layer thickness was estimated to be about 63 Å from the oxide capacitance measurement in the strong accumulation region at high frequency (1MHz). The sample temperature was always monitored by using a copper-constantan thermocouple close to the sample and measuring with a dmm/scanner Keithley model 199 and a Lake Shore model 321 auto-tuning temperature controllers with sensitivity better than $\pm$ 0.1 K. All measurements were carried out with the help of a microcomputer through an IEEE-488 ac/dc converter card.

3. RESULTS AND DISCUSSIONS

3.1. Temperature dependence of the forward bias I-V characteristics

The current-voltage (I-V) measurements of the Al/GaN/p-GaAs (MIS) Schottky diodes were performed in the temperature range of 80-380 K . For a MIS Schottky diode, it is assumed that the current of the device is due to TE theory and it can be expressed as [1,2]

$$I = I_o \exp\left(\frac{qV}{nkT}\right)\left[1 - \exp\left(-\frac{qV}{kT}\right)\right] \qquad (1)$$

where I_o is the reverse saturation current derived from the forward bias semi-logarithmic lnI-V plots and expressed as

$$I_o = A\,A^*\,T^2\,\exp\left(-\frac{q\Phi_{B0}}{kT}\right) \qquad (2)$$

where q is the electronic charge, A^* is the effective Richardson constant and equals 74.4 A cm^{-2}K^{-2} for p-type GaAs [25], A is the effective diode area, k is the Boltzmann constant, T is the temperature in K, Φ_{Bo}(I-V) is the zero bias barrier height and n is the ideality factor. The ideality factor is calculated from the slop of the linear region of the forward bias ln(I)-V plots and can be written from Eq.(1) as

$$n = \frac{q}{kT}\left(\frac{dV}{d(\ln I)}\right) \qquad (3)$$

The zero-bias barrier height Φ_{B0} (= Φ_B(I-V)) is determined from the extrapolated I_o and is given by

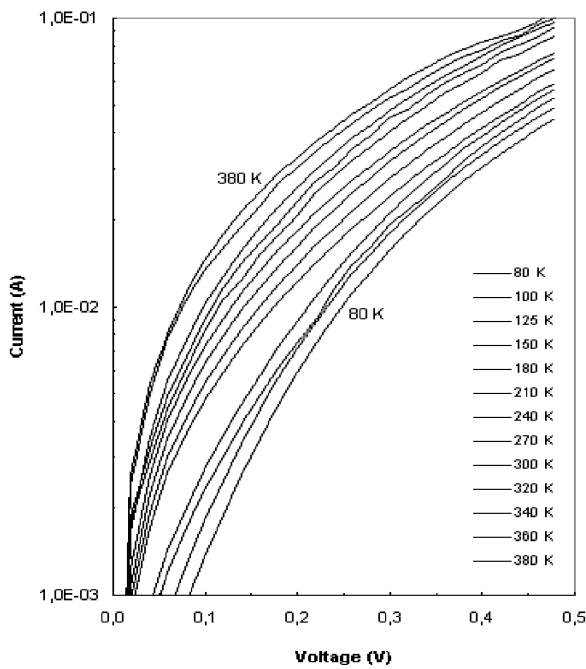$$\Phi_{B0} = \frac{kT}{q}\ln\left[\frac{AA^*T^2}{I_0}\right] \qquad (4)$$

FIG. 1: Experimental forward bias current-voltage (I-V) characteristics of the Al/GaN/p-GaAs (100) Schottky MIS diode at various temperatures.

FIG. 2: Temperature dependency of the ideality factor for Al/GaN/p-GaAs (100) Schottky MIS diodes.

FIG. 3: Temperature dependency of Φ_{B0} (I-V) obtained from I-V characteristics for Al/GaN/p-GaAs (100) Schottky MIS diodes.

The forward bias semi-logarithmic lnI-V characteristics for Al/GaN/p-GaAs Schottky diode in the temperature ranging from 80 K to 380 K are shown in Fig. 1. The I-V plots shift towards the higher bias side with decreasing temperature. The experimental values of the barrier height Φ_{B0} and the ideality factor n for the devices were determined from intercepts and slopes of the forward-bias ln(I) versus V plot at each temperature, respectively. The values of n and Φ_{Bo} were calculated from Eq.(3) and (4), respectively, at each temperature and shown in Table 1 and Figs. 2 and 3, respectively. As shown in Table 1, the experimental values of Φ_{B0} and n for the Al/GaN/p-GaAs (100) Schottky diodes ranged from 0.562 eV and 1.64 (at 380 K) to 0.115 eV and 8.16 (at 80 K), respectively. The Al/GaN/p-GaAs Schottky diode with the ideality factor value of 2.39 at 300K obey a metal-insulator layer-semiconductor (MIS) structure. This ideality factor value is significantly larger than an ideality Schottky diode. Such behavior of ideality factor has been attributed to particular distribution of interface states and insulator layer between metal and semiconductor [4,15]. This indicates that formed of an insulator layer (GaN) on the p-GaAs surface. Also, the values of ideality factor n was found to increase, while the Φ_{B0} decrease with decreasing temperature, as can be seen Figs. 2 and 3, respectively.

As explained in refs.[11,17,26-30], since the current transport across the metal-semiconductor (MS) interface is a temperature-activated process; electrons at low temperatures are able to surmount the lower barriers. Therefore, the current transp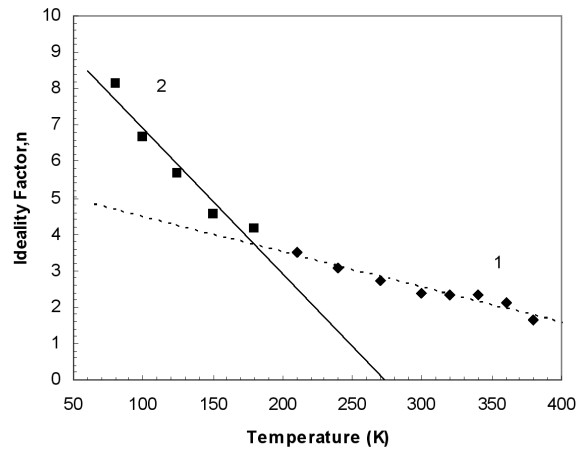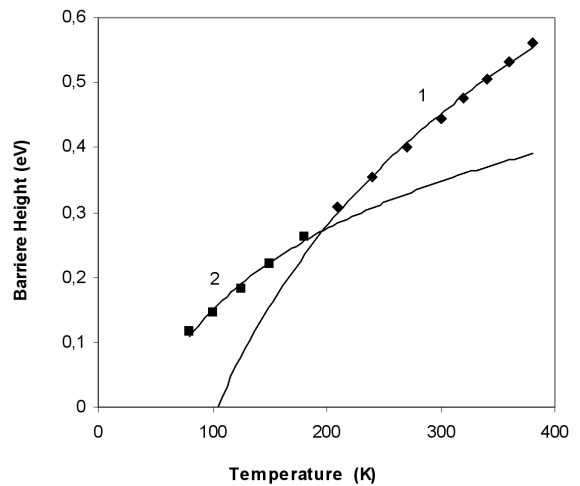ort will be dominated by the current flowing through the patches of lower Schottky barrier height (SBH), leading to a larger ideality factor. In other words, more and more electrons have sufficient energy to overcome the higher barrier build up with increasing temperature and bias voltage. An apparent increase in the ideality factor and a decrease in the barrier height at low temperatures are caused possibly by other effects such as non-uniformity of thickness and the interfacial charges.

3.2. Barrier heights inhomogeneities

The thermionic emission (TE) theory has normally been used to extract the Schottky diode parameters [14,15,26,31-33]. However, there have been several reports of certain anomalies [14,15,26,31,32] at low temperature. Generally, it is found that the ideality factor of a diode increases,

TABLE I: Temperature dependent values of various parameters determined from I-V characteristics of Al/GaN/p-GaAs(100) Schottky MIS diodes in the temperature range of 80-380 K.

T(K)	80	100	125	150	180	210	240	270	300	320	340	360	380
n	8.16	6.67	5.69	4.55	4.15	3.52	3.06	2.73	2.39	2.35	2.32	2.10	1.64
Φ_{B_0}	0.115	0.145	0.182	0.221	0.261	0.308	0.354	0.401	0.444	0.475	0.504	0.532	0.562

while the Φ_{B0} decreases with decreasing temperature [20] and this behaviour lead to nonlinearity in the activation energy plot. Here, we show the conventional energy variation of $\ln(I_o/T^2)$ versus $1/T$ for Al/GaN/p-GaAs metal-insulator-semiconductor MIS Schottky barrier diodes. According to Eq.(2), one obtains

$$\ln\left(\frac{I_0}{T^2}\right) = \ln\left(AA^*T^2\right) - \frac{q\Phi_{Bo}}{kT} \qquad (5)$$

The temperature dependency of experimental $\ln(I_o/T^2)$ versus $1/T$ plot was found to be non-linear in the temperature range measured (not shown here). The deviation in the Richardson plots may be due to the spatial inhomogeneities of the barrier height and potential fluctuations at the interface that consist of low and high barrier areas [9-12,16,18,20,26,33-35]. That is, the carrier transport mechanism across MS contact would flow preferentially through the lower barriers in the potential distribution [9-12,16,18,20,33-35]. As was explained by Horvath [28], the A^* value obtained from the temperature dependency of the I-V characteristics may be affected by the lateral inhomogeneity of the barrier.

The commonly observed deviation of classical thermionic emission theory can be explained by a recent model based on the assumption of a spatial fluctuation of the BH at interface. Namely, depending on temperature, the observed changes may be interpreted satisfactorily by incorporation of the concept of barrier inhomogeneities into thermionic emission theory [30]. In a real Schottky diode, the barrier height may not be the same over the entire area of contact due a variation in the thickness and/or composition of the interfacial layer and non-uniformity of the interfacial charges, etc [22,33].The barrier inhomogeneity approach mainly assumes that there is a distribution of barrier heights over the rectifying contact. Various types of distribution functions are suggested for describing barrier height inhomogeneities, for example Gaussian [16,22,23] and log-normal [49].

In order to explain the abnormal behavior between the theoretical and experimental values of Richardson constant A*, let us assume a barrier height with a mean value $\bar{\Phi}_{B0}$ and standard deviation σ_s, which can be given as [1,10-12,15,17,18].

$$P(\Phi_B) = \frac{1}{\sigma_s\sqrt{2\pi}}\exp\left[-\frac{(\Phi_B - \bar{\Phi}_B)^2}{2\sigma_s^2}\right] \qquad (6)$$

where $1/\sigma_S\sqrt{2\pi}$ is the normalization constant of the Gaussian barrier height distribution. Under forward bias, the total current I(V) across a Schottky diode containing barrier inhomogeneities can be expressed as

$$I(V) = \int_{-\infty}^{+\infty} I(\Phi_B, V)P(\Phi_B)d\Phi \qquad (7)$$

where $I(\Phi_B,V)$ is the current at a bias V for a barrier height based on the ideal thermionic-emission-diffusion (TED) theory and $P(\Phi_B)$ is the normalized distribution function giving the probability of accuracy for barrier height.

Now, introducing $I(\Phi_B,V)$ and $P(\Phi_B)$ from Eq.(1) and (6) into Eq.(7), and performing integration from -∞ to + ∞, one can obtain the current I(V) through a Schottky barrier at a forward bias V, similar to Eq.(1) and (2) but with the modified barrier

$$I(V) = AA^*T^2\exp\left[-\frac{q}{kT}\left(\bar{\Phi}_B - \frac{q\sigma_s^2}{2kT}\right)\right]$$

$$\exp\left(\frac{qV}{n_{ap}kT}\right)\left[1 - \exp\left(-\frac{qV}{kT}\right)\right] \qquad (8)$$

with

$$I_o = A\,A^*\,T^2\exp\left(-\frac{q\Phi_{ap}}{kT}\right) \qquad (9)$$

where Φ_{ap} and n_{ap} are the apparent barrier height and apparent ideality factor, respectively Φ_{ap} is given by [14,18],

$$\Phi_{ap} = \bar{\Phi}_{B0}(T = 0) \; - \; \frac{q\sigma_s^2}{2kT} \qquad (10)$$

The temperature dependency of σ_s is usually small and can be neglected [33]. In addition, the observed variation of the apparent ideality factor n with temperature T in the model is given by [16].

$$\left(\frac{1}{n_{ap}} - 1\right) = \rho_2 - \frac{q\rho_3}{2kT} \qquad (11)$$

It is assumed that the mean SBH,$\bar{\Phi}_B$, and σ_s are linearly bias dependent on Gaussian parameters, such as $\bar{\Phi}_B = \bar{\Phi}_{B0} + \rho_2 V$ and standard deviation $\sigma_s = \sigma_{so} + \rho_3 V$, where ρ_2 and ρ_3 are voltage coefficients which may depend on temperature, quantifying the voltage deformation of the BH distribution [17,18,20,36]. It is obvious that the decrease of zero-bias barrier height is caused by the existence of the Gaussian distribution, and the extent of influence is determined by the standard deviation itself. Also, the effect is particularly significant at

low temperatures. Fitting of the experimental data in Eq.(2) or (9) and in Eq.(3) gives Φ_{ap} and n_{ap}, respectively, which should obey Eq. (10) and (11).

The continuous curves in Figs. 2 and 3 and the linearity of the apparent barrier height and ideality factor versus q/2kT curves in Figs. 4 and 5 show that the temperature dependence experimental data of Al/GaN/p-GaAs (100) Schottky contact are in agreement with the recent model which is related to thermionic emission over a Gaussian BH distribution. Thus, the plot of Φ_{ap} versus q/2kT (Fig. 5) is expected to be a straight line with the intercept at the ordinate determining the zero-bias mean BH $\bar{\Phi}_{B0}$ and the slope giving the zero-bias standard deviation σ_s. The experimental Φ_{ap} versus q/2kT and n_{ap} versus q/2kT plots (Figs. 4 and 5) drawn using the data obtained from Fig. 1 respond to two lines instead of a single straight line with transition occurring at 180 K. These two different slopes at the lower and higher temperatures indicate two activated process with different mean barrier heights. The above observations show the existence of two Gaussian distributions of barrier heights in the contact area. Two sets of values of $\bar{\Phi}_{B0}$ and σ_s are obtained from the intercepts and slopes of these straight lines as 0.854 eV and 0.142 V in the temperature range of 210-380 K (distribution 1), and as 0.395 eV and 0.059 V in the temperature range 80-180 K (distribution 2). Moreover, the values of Φ_{ap} estimated from equation (4) over the entire temperature range curves 1 and 2 can be seen in Fig. 3. The existence of a double Gaussian in the metal-semiconductor (MS) contacts can be attributed to the nature of their inhomogeneities in the two cases. This may involve variation in the interface composition/phase, interface quality, electrical charges, nonstoichiometry, etc.. They electrically influence the I-V characteristics of the Schottky diodes, at particularly low temperatures. Hence, I-V measurements at very low temperatures can show the nature of barrier inhomogeneties existing in the contact area. That is, the presence of a second Gaussian distribution at very low temperatures may possibly occur due to some phase change taking place on cooling below a certain temperature. Furthermore, the temperature range covered by each straight line suggests the regime where the corresponding distribution is effective [30,33].

The above results have shown that the I-V-T characteristics of the Al/GaN/p-GaAs SBDs can be successfully explained on the basis of TE mechanism with a double Gaussian distribution of the barrier heights.

The plot of n_{ap} vs q/2kT should be a straight line that gives voltage coefficients ρ_2 and ρ_3 from the intercept and slope, respectively (Fig. 5). The values of ρ_2 obtained from the intercepts of the experimental n_{ap} vs q/2kT plot (Fig. 5) are -0.154 V in 210-380 K range (distribution 1) and -0.643 V in 80-180 K range (distribution 2), whereas the values of ρ_3 from the slopes are - 0.0213 V in 210 - 380 K range and - 0,0034 V in 80 - 180 K range. The linear behavior of this plot demonstrates that the ideality factor does indeed express the voltage deformation of the Gaussian distribution of the Schottky BH. According to these results, this inhomogeneity and potential fluctuation dramatically affect low temperature I-V characteristics.

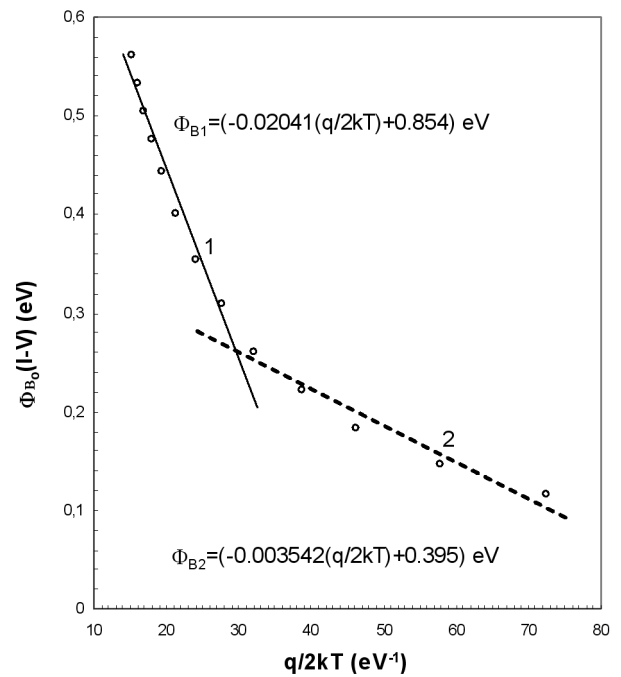The computed values exactly coincide with the experimen-

FIG. 4: The zero-bias apparent barrier height (Φ_{B0} (I-V)) versus q/2kT plot for Al/GaN/p-GaAs(100) Schottky MIS diode according to double Gaussian distribution.
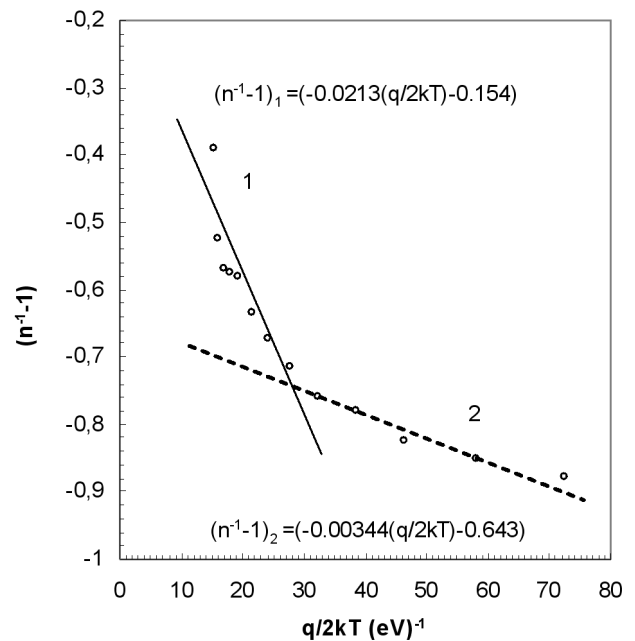
FIG. 5: The ideality factor ((n^{-1}-1)) versus q/2kT plot for Al/GaN/p-GaAs (100) Schottky MIS diode according to double Gaussian distribution.

tal results in the respective temperature ranges for two different distributions. As can be seen from the n_{ap} vs q/2kT plot, ρ_3 value or the slope of the distribution 1 is larger than that of distribution 2. Therefore, the distribution 2 at very low temperatures may possibly take place due to some phase change on cooling below a certain temperature.
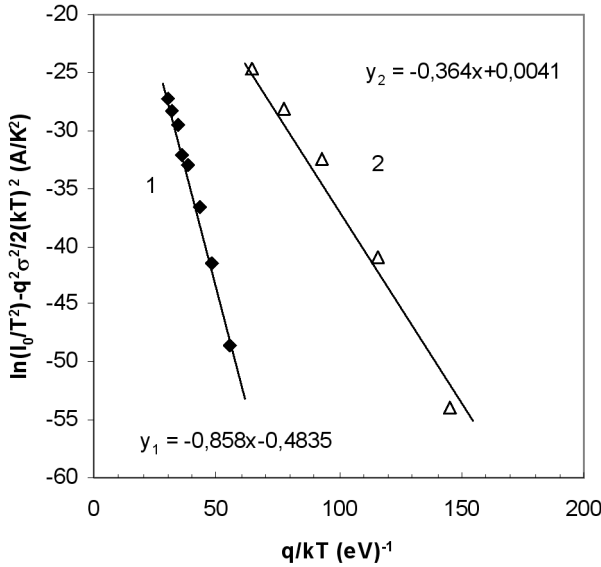

FIG. 6: Temperature dependence of $\ln(I_o/T^2)$-$q^2\sigma_0^2/2(kT)^2)$ versus q/kT for Al/GaN/p-GaAs (100) Schottky MIS diodes.

The conventional Richardson plot is now modified by combining Eqs. (10) with (11) as follows

$$\ln\left(\frac{I_0}{T^2}\right) - \left(\frac{q^2\sigma_o^2}{2k^2T^2}\right) = \ln(AA*) - \frac{q\bar{\Phi}_{B0}}{kT} \qquad (12)$$

The plot of a modified $\ln(I_0/T^2)$ - $q^2\sigma_o^2/2k^2T^2$ vs q/kT according to Eq.(12) should give a straight line with the slope directly yielding the mean $\bar{\Phi}_{B0}$ and the intercept (=lnAA*) at the ordinate determining A* for a given diode area A. Fig. 6 shows this plot.

The $\ln(I_o/T^2)$ - $q^2\sigma_o^2/2k^2T^2$ values were calculated for both values of σ_o obtained for the temperature range of 80-180 K and 210-380 K. The open triangles and closed squares in Fig. 6 have given the modified $\ln(I_0/T^2)$ - $q^2\sigma_o^2/2k^2T^2$ vs q/kT plots for both values of σ_o and zero-bias mean BH $\bar{\Phi}_{B0}$ obtained 0.364 eV in 80-180 K range (distribution 2)

and 0,858 eV in 210-380 K range (distribution 1). These values match exactly with the mean BHs obtained from the Φ_{ap} versus q/2kT plots in Fig. 6. The intercepts at the ordinate give the Richardson constant A* as 128 A/cm²K² in 80-180 K range and 78.5 in 210-380 K range without using the temperature coefficient of the BHs. The Richardson constant value of 78,5 A/cm²K² for the range of 210-380 K is almost the same as the value of 74.4 A/cm²K² known for holes in p-type GaAs. As can be seen, the values of $\bar{\Phi}_{B0}$ 0.858 eV and 0.364 eV from this plot is in close agreement with the values of $\bar{\Phi}_{B0}$ 0.854 eV and 0.395 eV from the plot of Φ_{ap} versus q/2kT.

4. CONCLUSION

Current-voltage (I-V) characteristics of Al/GaN/p-GaAs SBDs were measured in the temperature range of 80-380 K. The results underline the importance of investigations in a wide temperature range since I-V measurements at room temperature alone do not provide satisfactory insights. The experimental results have showed the non-ideal behavior of the current-transport over the barrier expressed by ideality factors, significantly larger than unity at lower temperatures and an increasingly effective SBH with rising temperature. The high value of *n* is attributed to the potential drop in the interfacial insulator layer and recombination through the interface states. In order to obtain evidence of single or double/multiple Gaussian distribution of the BHs, we have drawn Φ_{ap} vs q/2kT plot. We obtained two straight lines with negative slope for double Gaussian distribution of BHs. While the slope of each straight line gives the standard deviation, the intercept at the ordinate yields the mean of the Gaussian distribution. Then, the values of Richardson constant A* were obtained from a modified $\ln(I_0/T^2)$-$q^2\sigma_o^2/2(kT)^2$ vs q/kT plot as 128 A/cm²K² in 80-180 K and 78.5 A/cm²K² in 210-380 K. It has been concluded that the I-V-T characteristics of Al/GaN/p-GaAs SBDs can be satisfactorily explained on the bases of TE mechanism with two Gaussian distributions of the Schottky barrier heights in the temperature range of 80-380 K. In this study has not been described in detail of properties of nitridation layer (GaN). However, in this study indicates existence of an insulator layer (GaN) because the behavior of ideality factor and double Gaussian distribution of barrier height has been attributed insulator layer between metal and semiconductor.

[1] S. M. Sze, *Physics of Semiconductor Devices*, 2nd Edn. Willey, New York 1981, p.850.

[2] E. H. Rhoderick, R. H. Williams, *Metal-Semiconductor Contacts,* 2nd Ed. Clarendon Press, Oxford, 1988.

[3] C. R. Crowell and S. M. Sze, J. Appl. Phys. **36**, 3212 (1965).

[4] H. C. Card, E. H. Rhoderick, J. Phys. D: Appl. Phys. **4**, 1589 (1971).

[5] A. Singh, K. C. Reinhardt, and W. A. Anderson, J. Appl. Phys.

68(7), 3475 (1990).

[6] P. Cahttopadhyay, A. N. Daw, Solid-State Electron. **29**, 555 (1986).

[7] P. Cova and A. Singh, Solid-State Electron. **33**, 11 (1990).

[8] M. O. Aboelfotoh, J. Appl. Phys. **69**, 3351 (1991).

[9] Ş. Karataş, Ş. Altındal, A. Türüt, and A. Özmen, Appl. Surf. Sci. **217**, 250 (2003).

[10] M. K. Hudait, P. Venkateswarlu, and S. B. Krupanidhi, Solid-State Electron. **45**, 133 (2001).

[11] S. Chand, Semicond. Sci. Technol. **19**, 82 (2004).

[12] S. Zhu, R. L. Van Meirhaeghe, C. Detavernier, G. P. Ru, B. Z. Li, and F. Cardon, Solid-State Comm. **112**, 611 (1999).

[13] J. P. Sullivan, R. T. Tung, M. R. Pinto, and W. R. Graham, J. Appl. Phys. **70**, 7403 (1991).

[14] B. Akkal, Z. Benemara, A. Boudissa, N. B. Bouiadjra, M. Amrani, L. Bideux, and B. Gruzza, Mater. Sci. And Eng. B, **55**, 162 (1998).

[15] Ş. Altındal, S. Karadeniz, N. Tuğluoğlu, and A. Tataroğlu, Solid-State Electron. **47**, 1847 (2003).

[16] J. H. Werner and H. H. Güttler, J. Appl. Phys. **69**, 1522 (1991).

[17] S. Zeyrek, Ş. Altındal, H. Yüzer, and M. M. Bülbül, Appl. Surf. Sci. **252**, 2999 (2006).

[18] S. Zhu, R. L. Van Meirhaeghe, C. Detavernier, F. Cardon, G. P. Ru, X. P. Qu, and B. Z. Li, Solid-State Elecron. **44**, 663 (2000).

[19] S. Hardikar, M. K. Hudait, P. Modak, S. B. Krupanidhi, and N. Padha, Appl. Phys. A **68**, 49 (1999).

[20] A. Gümüş, A. Türüt, and N. Yalçın, J. Appl. Phys.**91**, 245 (2002).

[21] K. Yasui, T. Arayama, S. Okutani, and T. Akahane, Appl. Surf. Sci. **212-213**, 619 (2003).

[22] Y. P. Song, R. L. Van Meirhaeghe, W. H. Laflere, and F. Cardon, Solid-State Electron. **29**, 633 (1986).

[23] P. G. McCafferth, A. Sellai, P. Dawson, and H. Elabd, Solid-State Electron. **39**, 583 (1996).

[24] V. L. Berkovits, T. V. L'vova, and V. P. Ulin, Vacuum **57**, 201 (2000).

[25] E. Hökelek, Y. Robinson, Solid-State Electron. **24**, 99 (1981).

[26] Ş. Karataş, Ş. Altındal, and M. Çakar, Physica B **357**, 386 (2005).

[27] A. Türüt, N. Yalçın, and M. Sağlam, Solid-State Electron. **35**, 835 (1992).

[28] Zs. J. Horvarth, Solid-State Electron. **39**, 176 (1996).

[29] F. A. Padovani, R. Stratton, Solid-State Electron. **9**, 695 (1966).

[30] A. F. Özdemir, A. Türüt, A. Kökçe, Semicond. Sci. Technol. **21**, 298 (2006).

[31] A. S. Bhuiyan, A. Martinez, and D. Esteve, Thin Solid Films **161**, 93 (1988).

[32] Ş. Karataş and A. Türüt, Physica B **381**, 199 (2006).

[33] S. Chand and J. Kumar, Semicond. Sci. Technol. **11**, 1203 (1996).

[34] S. Chand and J. Kumar, Appl. Phys. A. **65**, 497 (1997).

[35] K. Maeda, Surf. Sci. **493**, 644 (2001).

[36] S. Zhu, C. Detavernier, R. L. Van Meirhaeghe, F. Cardon, G. P. Ru, X.P. Qu, and B. Z. Li, Solid-State Electron. **44**, 1807 (2000).

[37] H. Yüzer, H. Doğan, J. Köroğlu, and S. Kocakuşak, Spectrochimica Acta Part B **55**, 991 (2000).

[38] X. Y. Hou, W. Z. Cal, Z. Q. He, P.H. Haı, Z. S. Li, X. M. Ding, and X. Wang, Appl. Phys. Lett. **60**, 2252 (1992).

[39] H. Sik, Y. Feurprier, C. Cardinaud, G. Turban, and A. Scavennec, J. Electrchem. Soc. **114**, 2106 (1997).

[40] K. Tsuchiya, M. Sakata, A. Funyu, and H. Ikoma, J. Appl. Phys. **34**, 5926 (1995).

[41] V. L. Berkovits, T. V. L'vova, and V. P. Ulin, Vacuum **57**, 201 (2000).

[42] J. Riikonen, J. Sormunen, H. Koskenvaara, M. Matilla, M. Sponen, and H. Lipsanen, J. Crys. Grow. **272**, 621 (2004).

[43] K. Yasui, T. Arayama, S. Okutani, and T. Akahane, Appl. Surf. Sci. **212-213**, 619 (2003).

[44] Y. G. Li, A. T. S. Wee, C. H. A. Huan, and J. C. Zheng, Appl. Surf. Sci. **174**, 275 (2001).

[45] K. Yasui, T. Arayama, S. Okutani, and T. Akahane, Appl. Surf. Sci. **175-176**, 585 (2001).

[46] J. Lu, D. I. Westwood, L. Haworth, P. Hill, and J. E. Macdonald, Thin Solid Films **343-344**, 567 (1999).

[47] Y. Ould-Metidji, L. Bideux, D. Baca, B. Gruzza, and V. Matolin, Appl. Surf. Sci. **212-213**, 619 (2003).

[48] S. S. Hullavarad, S. V. Bhoraskar, S. R. Sainkar, S. Badrinarayanan, A. B. Mandale, and V. Ganesan, Vacuum. **55**, 121 (1999).

[49] Z. J. Horwath, Mater. Res. Soc. Symp. Proc. **260**, 367 (1992).

[50] M. A. Ebeoğlu, Physica B **403**, 61 (2008).